Published in final edited form as:
Atherosclerosis. 2011 August ; 217(2): 387–394. doi:10.1016/j.atherosclerosis.2011.06.015.

Genetical genomics of Th1 and Th2 immune response in a baboon model of atherosclerosis risk factors

A Vinson[a,b], **JE Curran**[c], **MP Johnson**[c], **TD Dyer**[c], **EK Moses**[c], **J Blangero**[c], **LA Cox**[c,d], **J Rogers**[c,d], **LM Havill**[c], **JL VandeBerg**[c,d], and **MC Mahaney**[c,d]

[a]Dept. of Molecular and Medical Genetics, Oregon Health & Science University, Portland, OR

[b]Oregon National Primate Research Center, Beaverton, OR

[c]Dept. of Genetics, Southwest Foundation for Biomedical Research, San Antonio, TX

[d]Southwest National Primate Research Center, San Antonio, TX

Abstract

Objective—CD4$^+$ T-cells mediate inflammation in atherosclerosis, but additive genetic effects on associated pathways of Th1 and Th2 immune response have not been described. We sought to characterize heritability, pleiotropy, and QTL effects on the expression of genes implicated in Th1 and Th2 immune response in a baboon model of risk factors for atherosclerosis.

Methods—We employed a maximum likelihood-based variance decomposition approach to estimate additive genetic effects on transcript levels generated from a gene expression profile of lymphocytes in 499 pedigreed baboons maintained on a basal diet. Transcript levels for 57 genes implicated in Th1 and Th2 immune response were selected for analysis based on significant heritability in this profile. Multipoint whole genome scans were conducted on heritable transcript levels to localize QTLs influencing these measures. To evaluate pleiotropic effects on transcript levels, we estimated genetic and phenotypic correlations among transcript measures, and assessed their correspondence using a Mantel test. Network analysis using GeneGo's MetaCore™ software was conducted to characterize known interaction among coded proteins.

Results—Heritabilities for candidate gene transcript levels ranged from 0.092— 0.786 (median h^2=0.278, P=4.72× 10^{-4}). Linkage analyses yielded significant evidence (LOD≥2.73) for 14 eQTLs (LOD score range 2.76—14.87, genome-wide P=4.9 × 10^{-2}—1.03 × 10^{-14}). Estimates of genetic correlation supported shared additive genetic effects incorporating all 57 transcripts (null hypothesis of ρ_G= rejected at FDR≤0.05 for 522 of 1,596 estimates), and accounted for most of the observed phenotypic correlation among transcripts (Mantel test, $r_{[\rho P],[\rho G]}$=0.781, P<0.0001). Network analysis revealed direct interactions among 54 of the 57 coded proteins.

Conclusions—We conclude that major genetic effects influence expression levels of multiple genes implicated in Th1 and Th2 immune response. Additionally, we find that expression levels of

CORRESPONDING AUTHOR: Amanda Vinson, Ph.D., Dept. of Molecular and Medical Genetics, Oregon Health and Science University, 3181 SW Sam Jackson Park Rd., Mail code L103A, Portland, OR. 97239, PH: (503) 418-8391, FX: (503) 494-4411, vinsona@ohsu.edu.

Financial Disclosures: None.

Conflict of interest: The authors declare no conflict of interest.

these candidate genes are characterized by extensive pleiotropy, consistent with known interaction among their coded proteins, many of which are independently associated with atherosclerosis.

Keywords

QTL; Th1; Th2; gene expression; atherosclerosis; baboon; inflammation

Introduction

Considerable evidence from patient-based studies of atherosclerosis and in experimental models of disease indicates that activated $CD4^+$ T cells modulate inflammation at multiple stages of plaque development and progression. In emerging lesions, $CD4^+$ T cells home to sites of endothelial disturbance and migrate into the arterial intima, where they are activated by specific antigens. These cells are characterized phenotypically and functionally as effector T-helper cells, and serve to activate other immune cells that may continue to drive inflammation in the lesion (reviewed in [1]). Notably, activated T cells are expanded in complicated human atheromata[2,3] and in the periphery of patients presenting with acute coronary syndrome (ACS)[4-6], findings that implicate these cells in the instability that characterizes plaques prone to rupture, with accompanying thrombosis and myocardial infarction.

Pro-inflammatory T-helper 1 (Th1) effector cells are found in emerging (fatty streak) atherosclerotic lesions[7], and are key mediators of inflammation in the developing plaque. Th1 cells promote inflammation by proliferating in response to antigens present in the lesion (e.g., modified lipoproteins or bacterial and viral antigens), and secreting cytokines that activate macrophages and other cell types[1]. Cytokines associated with a Th1 immune response include the signature Th1 cytokine interferon-gamma (IFNγ), TNF family members TNFα and lymphotoxin (TNFβ), and IL-12, IL-15, and IL-18, which may further stimulate Th1 response by increasing IFNγ expression[1,8-9]. The production of IFNγ results in a cascade of pro-inflammatory and atherogenic effects. IFNγ stimulates increased expression of cell adhesion molecules on the endothelial cell surface, increasing the attraction of additional T-cells to the developing lesion[1]. IFNγ also upregulates scavenger receptor expression on macrophages, and expression of the MHC Class II molecules HLA-DQ on vascular smooth muscle cells and HLA-DR on macrophages and vascular smooth muscle cells, allowing these cells to present antigen to T-cells[10]. Moreover, IFNγ upregulates the expression of multiple co-stimulatory molecules required for continued T-cell activation[1]. Consistent with these findings, Th1-associated cytokines are found in murine fatty streak lesions (IFNγ and lymphotoxin)[7,11], and Th1 cell numbers are positively associated with size of murine fatty streak lesions[7].

Evidence suggests that Th1 effector cells increase in number during the transition from fatty streak to a more complicated atheroma, and act to enhance the susceptibility of the lesion to rupture[1,3,12]. Significant numbers of T cells are found in the fibrous cap of atherosclerotic plaques, with a substantial proportion bearing markers of activation[3,13-14]. Activated T-cells surrounded by IFNγ are found in human atheromata collected at endarterectomy[3], increase in frequency with severity of disease[2], and are located at the point of rupture in lesions resulting in fatal myocardial infarction[14]. These findings are consistent with progressive effects of IFNγ, both direct and indirect, that erode the protective fibrous cap present in the lesion. IFNγ directly inhibits vascular smooth muscle cell proliferation and collagen synthesis in the lesion, leading to thinning and instability of the fibrous cap[1,15]. IFNγ also upregulates inflammatory molecules (e.g., reactive oxygen species, proteases, coagulation factors, and multiple other pro-inflammatory cytokines and chemokines) in other cell types that also act to degrade the fibrous cap of the lesion[1].

In agreement with these findings, a dominant Th1 immune response is associated with advanced atherosclerosis in humans and in experimental models of human disease[16-18]. Cytokines associated with a Th1 immune response are present in human and murine atheromata (IFNγ, lymphotoxin, IL-12p40, IL-12p70, and IL-18)[8,11,17,19-20], and are implicated in disease progression, as evidenced by accelerated atherosclerosis with IL-12 administration in mice[20], and association of circulating IL-18 with advanced heart failure in humans[21]. The presence of these cytokines in advanced disease is consistent with the significantly increased numbers of peripheral activated T cells (i.e., $CD3^+CD69^+$, $CD3^+HLA\text{-}DR^+$) found in patients with coronary artery disease (CAD), compared to healthy controls[6]. Further, in a finding that underscores the role of Th1 cells in decreasing the stability of advanced lesions, patients presenting with ACS, including unstable angina[4-5] and ST-segment elevation myocardial infarction[4], exhibited a significant expansion of peripheral Th1 cells (i.e., $CD3^+IFN\gamma^+$; $CD3^+CD4^+IFN\gamma^+$)[4-5] compared to patients with extensive but stable disease, accompanied by corresponding increases in peripheral expression of soluble STAT4 (a Th1-associated transcription factor), IL-2, and IFNγ[4].

In contrast to the pro-inflammatory Th1 effector cell, the T-helper 2 (Th2) cell has been associated with attenuated inflammation in atherosclerosis. The differentiation of Th2 cells both depends on and results in the further production of IL-4, the signature cytokine of the Th2-mediated response, although Th2 cells also produce IL-5, IL-10, and IL-13[22] (reviewed in [23]). Cytokines characteristic of a Th2-mediated response may inhibit production of IFNγ, down-regulate Th1 differentiation, or have other antiinflammatory effects that inhibit Th1 response and atherogenesis[23-24]. Evidence consistent with anti-atherogenic effects of Th2 cytokines includes decreased lesion size in mice with administration of IL-4[7], accelerated atherosclerosis with IL-5 deficiency in mice[25], and the association of IL-10 with down-regulation of IFNγ and decreased lesion formation in mice[24], and with down-regulation of IL-12 in humans[19]. Production of Th2 cytokines in T cell clones from human atheromata is limited, suggesting the relative rarity of Th2 cells in atherosclerotic lesions[16-17].

Although substantial evidence indicates that $CD4^+$ effector T cells modulate inflammation in atherosclerosis, the extent of genetic effects influencing these pathways has not been described. In this study, we characterize additive genetic effects on pathways of T-helper cell immune response in the baboon, an important model of atherosclerosis risk factors, a) by reporting significant heritability for transcript levels of 57 candidate genes implicated in multi-cellular pathways of human Th1 and Th2 cell activation, differentiation, and cytokine signaling; b) by localizing quantitative trait loci (QTLs) influencing these candidate gene transcript levels, and c) by assessing the extent of genetic effects shared among transcript levels, and the relationship of these shared genetic effects to observed co-variation among transcripts and coded proteins.

Materials and Methods

Animals

We obtained data for this study from a sample of 499 baboons (*Papio hamadryas*, 373 females and 126 males) that form part of a large pedigreed and genotyped population used successfully for >30 years to study the interaction of diet and genotype in characterizing risk factors for atherosclerosis. Baboons are maintained outdoors in social groups at the Southwest National Primate Research Center/Southwest Foundation for Biomedical Research (SNPRC/SFBR) in San Antonio, Texas, and range in age from 6 to 34 years, corresponding developmentally to an age range of 18—102 years in humans. Animal care personnel and staff veterinarians provided routine and emergency health care to all animals in accordance with the Guide for the Care and Use of Laboratory Animals. The SFBR facility is certified by the Association for Assessment and Accreditation of Laboratory

Animal Care International, and all procedures were approved by the Institutional Animal Care and Use Committee. Baboons sampled in this study had *ad libitum* access to a low-fat, low cholesterol commercial monkey diet (basal diet, SWF Primate Diet; Harlan Teklad, Madison, WI).

Measures of transcript abundance

Conservation of focal transcript sequences in human and baboon genome— Due to the current draft stage of the baboon genome, a comprehensive and well-annotated whole transcriptome assay for this species has not yet been developed. Based on our own successful use of human short tandem repeats (STRs) to map the baboon genome, as well as our considerable past success using human assays to measure cardiovascular risk factors in this species[S1-S3], we elected to use the Illumina HumanWG-6 Expression BeadChip to measure whole-genome gene expression in this study. To gauge the likely success of using this oligonucleotide-based assay in baboons, we assessed the extent of mRNA sequence conservation between both species for the set of candidate genes investigated in this study. Sequence archived in GenBank (http://www.ncbi.nlm.nih.gov/genbank/) was available for both human and baboon mRNA representing 6 of the 57 genes (*CD28*, *CD4*, *CD86*, *CTLA4*, *IFNG*, and *IL12B/IL12p40*); these sequences were downloaded and aligned using GeneDoc software[26]. Additionally, for 45 of the 57 genes, we used the "discontiguous megablast" algorithm with the nucleotide BLAST program (http://blast.ncbi.nlm.nih.gov/Blast.cgi) to interrogate Phase 2 and 3 sequences found in the *Papio hamadryas* high throughput genomic sequence database (HTGS; http://www.ncbi.nlm.nih.gov/HTGS/) with human mRNA sequence downloaded from GenBank.

In all, 48 of the 57 genes and transcripts investigated were analyzed for expressed sequence identity between baboons and humans, revealing an estimated mean identity of 96% (range 83% - 100%), weighted by number of nucleotides examined. These findings (and others described in the RESULTS section) indicate that DNA sequence is highly conserved between both species, and support the idea that transcript levels measured in this study are a reflection of biological reality, rather than a consequence of mismatches in probe sequence.

Data collection and pre-processing—Lymphocytes were extracted from whole blood collected in EDTA. Total RNA was isolated from these cells using a TRIzol (Invitrogen) RNA extraction protocol with a chloroform interphase separation and subsequent isopropanol and ethanol precipitation. Total RNA samples were air dried, resuspended in RNase-free water and stored at -80°C. Seven microliters of isolated total RNA was further treated to remove globin mRNA with the GLOBINclear® kit (Ambion, USA) according to the manufacturer's protocol. Purified total RNA yield (μg) and purity (260nm:280nm) were determined spectrophotometrically using the NanoDrop ND-1000 (Wilmington, DE). A total of 500ng total RNA was dried using an Eppendorf Vacufuge Concentrator 5301 (Eppendorf, Germany) and stored at -20°C prior to anti-sense RNA (aRNA) synthesis. Anti-sense RNA was synthesized, amplified and purified using the Ambion MessageAmp II Amplification Kit (Ambion, USA). Hybridization of aRNA to Illumina's HumanWG-6 v1.0 Expression BeadChips and subsequent washing, blocking and detection were carried out using Illumina's BeadChip 6×2 protocol[27]. Baboon lymphocyte samples were scanned on the Illumina BeadArray 500GX Reader using Illumina BeadScan image data acquisition software (version 2.3.0.13). Illumina BeadStudio software (version 1.5.0.34) was used for preliminary data analysis after correcting for background signal noise. Illumina Gene Expression BeadChips have internal control features to monitor data quality, and results of these controls were visualized using Illumina GenomeStudio™ software. This software includes routines for calculating and reporting a detection p-value that represents the confidence a given transcript is expressed above the background defined by the negative

control probes included on the BeadChips. Other controls include Illumina-supplied oligos randomly imbedded in the expression chip substrate to ensure adequate and specific hybridization of samples. A positive control RNA sample (Stratagene Universal RNA) was also included in each day's run to assess for abnormalities in the aRNA synthesis, amplification and purification procedures.

Each Illumina HumanWG-6 v1 Expression BeadChip contains 47,289 unique 50-mer oligonucleotides, of which 22,151 (47%) target Reference Sequence[28] transcripts and the remaining 25,128 probes (53%) target other, generally less well characterized transcripts, including predicted transcripts. To identify transcripts exhibiting sufficient quantitative expression in baboon lymphocytes to support further analyses, we compared the distribution of expression values for a given transcript to the distribution of the expression values of the controls imbedded in each chip. For each transcript, we conducted a χ^2 "tail" test to determine if there was a significant excess of samples with values above the 95th percentile of the null distribution based on manufacturer-provided negative control samples. Using a stringent false discovery rate (FDR) of 5%, we identified 15,683 transcripts that exhibited significant expression in baboon lymphocytes by this criterion.

To detect true biological differences between individual baboons, a series of standardization steps was used to make the expression phenotypes comparable across individuals and across transcripts, resulting in normally distributed expression phenotypes. To minimize the influence of overall signal levels, which may reflect RNA quantity and quality rather than true biological differences between individuals, we first standardized abundance values of all retained transcripts by z-scoring within individuals, using decile percentage bins of transcripts grouped by average log-transformed raw signals across individuals. We followed this with linear regression against individual-specific average log-transformed raw signal and its squared value. Lastly, for each transcript, we directly normalized these residual expression scores by employing an inverse Gaussian transformation across individuals, to ensure that the assumption underlying variance components-based analyses is not violated. This very conservative procedure results in normalized expression phenotypes that are comparable between individuals and across transcripts[27]. Using the same FDR of 5%, 10,719 of these transcripts (68.3%) exhibited significant heritability.

Baboon Pedigree and Whole Genome Linkage Map

Analyses of these traits took advantage of a baboon genome linkage map based on genotype data at nearly 300 microsatellite marker loci (mean inter-marker interval=8.9 cM) from 2,044 baboons placed in a single extended pedigree spanning 6 generations. The physical locations in the human genome for nearly all marker loci in the baboon map are known, facilitating the identification of orthologous chromosomal regions in the two species. Construction of the current baboon linkage map is described in detail elsewhere[29], and additional information can be found at the SNPRC website: http://baboon.sfbrgenetics.org/.

Statistical Genetic Methods

Heritability—We conducted all analyses using a maximum likelihood-based variance decomposition approach implemented in the software package SOLAR (Sequential Oligogenic Linkage Analysis Routines). This approach, described in detail elsewhere[30] partitions the phenotypic variance in each trait (σ_p^2) into components corresponding to additive genetic effects (σ_G^2), estimated as a function of relatedness among pedigreed baboons, and environmental effects (σ_E^2). After regressing out mean effects of age, age^2, and sex from standardized measures of transcript abundance, we assessed residuals for departures from multivariate normality[31], and applied an inverse Gaussian transformation to

correct for any such departure. We estimated heritability for these data as the proportion of residual phenotypic variance unexplained by covariates that can be attributed to additive genetic effects $(h^2=\frac{\sigma_G^2}{\sigma_p^2})$.

Pleiotropy—To determine the extent of additive genetic effects shared among transcript levels, we used a bivariate expansion of the variance decomposition model described above to estimate the additive genetic correlation (ρ_G) between all possible trait-pairs (this model additionally provides estimates of environmental correlation (ρ_E) among trait-pairs). We assessed the significance of estimates of ρ_G by means of likelihood ratio tests, which compare the likelihoods of models in which the correlation was estimated to those in which it was constrained to zero (rejection of $\rho_G=0$ indicates pleiotropy) or to 1 (failure to reject $|\rho_G|=1$ indicates complete pleiotropy). We corrected for multiple comparisons using the false discovery rate (FDR) of Benjamini and Hochberg[32], and considered as significant only those genetic correlations characterized by a FDR ≤ 0.05.

To investigate the extent to which patterns of phenotypic correlation (ρ_P) reflect patterns of genetic correlation between transcript levels for our focal gene set, we first estimated phenotypic correlations among all possible trait-pairs as $\rho_P=\rho_G\sqrt{h_1^2}\sqrt{h_2^2}+\rho_E\sqrt{1-h_1^2}\sqrt{1-h_2^2}$, using estimates of trait-specific heritability and genetic and environmental correlations among trait-pairs provided by the bivariate analysis described above. Using the Pearson product moment correlation (r) as an estimate of similarity, we conducted a Mantel test[33] that compared the matrices of these estimated genetic and phenotypic correlations using a routine implemented in XLSTAT (version 2008.6.04; http://www.xlstat.com/). The significance of the estimate of this correlation (for a two-tailed test with α=0.01) was obtained from the distribution of $r[\rho_P],[\rho_G]$ estimated from 100,000 permutations of matrix columns and rows.

Linkage—To assess whether major genetic effects on candidate gene transcript levels could be localized, we conducted univariate multipoint whole genome linkage analyses for each of the focal transcripts. Linkage models based on a variance decomposition approach partition the genetic covariance between relatives into locus-specific and residual genetic effects, using estimates of multipoint identity-by-descent (IBD) allele-sharing. Multipoint IBD allele-sharing among relatives is estimated throughout the baboon linkage map based on genotype data at the microsatellite markers, employing Markov Chain Monte Carlo routines implemented in the computer package Loki[34]. Based on these estimates of IBD, we tested linkage hypotheses at 1 cM intervals along each chromosome using likelihood ratio tests, and converted the resulting likelihood ratio statistic to the LOD score of classic linkage analysis[35]. To control for the genome-wide false positive rate, we calculated genome-wide P-values for each LOD score using a modification of a method suggested by Feingold et al.[36] that takes into account pedigree complexity and the finite marker density of the linkage map. Accordingly, our threshold for significant evidence of linkage (corresponding to genome-wide α=0.05) was LOD=2.73, while the threshold for suggestive evidence of linkage was LOD=1.50.

Network Analysis—To determine whether relationships among molecules coded by candidate genes were consistent with the patterns of genetic and phenotypic correlation observed in this study, we used the GeneGo MetaCore™ pathways analysis software (v.5.2, Build 17389) to build a network based on curated experimental evidence for relationships among the molecules of interest. Gene symbols for focal transcripts were uploaded as a list to the MetaCore™ portal. Using the direct-interactions network building algorithm,

interactions among gene products were diagrammed based on peer-reviewed experimental evidence culled by expert personnel following the GeneGo MetaCore approach (described in detail at http://www.genego.com/metacore.php).

Results

Transcript levels of 57 candidate genes were selected for analysis based on the reported role of the coding gene or gene product in pathways of Th1 and Th2 cell activation and function[S4-S22], and on their significant heritability in this study (h^2 range = 0.092—0.786, corresponding P-value range = 1.30×10^{-2}—3.42×10^{-23} (Table 1); transcript levels for an additional 53 genes initially examined were not characterized by significant heritability in this study). Employing a conservative FDR threshold of 0.05, bivariate analyses of all pairwise transcript measures produced 522 significant estimates of additive genetic correlation ranging from |0.41 -1.0| among 1,596 possible tests; significant results included interactions among all 57 transcript measures. Of note, this substantial degree of genetic correlation discovered among transcript levels offers further support for the biological reality of the transcript measures in this study, as the independent occurrence of mismatches in probe sequence between genes would likely preclude correlation among transcripts except that due solely to chance. Following the rule of thumb for interpreting linear correlations, these results indicate that from 17-100% of total additive genetic variance in transcript levels is shared among transcripts. As expected, the magnitude of these shared genetic effects contributed to a close correspondence between genetic and phenotypic correlation among transcript measures, to an extent estimated by the Mantel test of association ($r_{[\rho P], [\rho G]}$ = 0.781, P<0.0001), indicating that approximately 60% of the variance in these two matrices is shared.

Consistent with a close relationship between shared genetic and phenotypic effects on transcript levels, we found that published evidence (as curated by MetaCore personnel) supported direct interactions among virtually all proteins coded by the 57 candidate genes (FIGURE 1); CMIP, LAG3, and NFATC3 were added to this network via interactions with intermediary molecules. The greatest number of interactions were observed for IFNγ (37 edges) and IL-10 (21 edges), in agreement with their role as key pro- and anti-inflammatory cytokines in cross-regulatory Th1 and Th2 immune response, respectively. This network was most significantly associated with autoimmune disease ($P=1.52\times 10^{-34}$), type 1 diabetes ($P=7.39\times 10^{-31}$), and rheumatoid arthritis ($P=3.08\times 10^{-27}$).

Table 2 summarizes the results of linkage analyses reaching genome-wide statistical significance, including LOD scores, expression QTL (eQTL) heritability, implicated eQTL regions, and likely mode of regulation. Univariate linkage analyses yielded at least suggestive evidence for linkage (i.e., LOD≥1.50) for 43 of the 57 transcripts (results not shown for eQTLs with 1.50≥LOD≤2.73). Of these 43 eQTLs, 14 were supported by significant evidence for linkage (i.e., LOD≥2.73), with LOD scores ranging from 2.76 to 14.87, with corresponding genome-wide P-values ranging from 4.9×10^{-2} to 1.03×10^{-14}. The eQTL-specific heritabilities (i.e., the proportion of total phenotypic variation exhibited by transcript levels due to additive genetic effects at the eQTL) ranged from 0.228—0.600. For 9 of the 14 eQTLs supported by significant evidence for linkage, the eQTL accounted for all detectable additive genetic variation influencing transcript levels at the cM position corresponding to maximum linkage evidence.

We examined evidence for likely *cis*- and *trans*- effects of the eQTL on each transcript by identifying the region in the baboon genome surrounding the microsatellite markers containing LOD scores ± 1.5 from the maximum LOD score, and locating the corresponding physical region flanked by the same markers in the reference sequence of the human

genome. Of the 14 significant eQTLs, 8 localized to regions in the baboon genome orthologous to human genomic regions containing the gene coding for the measured transcript, while 6 eQTLs localized outside such regions.

Discussion

It is clear that for many genes implicated in T-helper immune response, expression levels in lymphocytes vary considerably among baboons, and additive genetic effects contribute to this inter-individual variation in gene expression. This finding is noteworthy because these traits were measured *in vivo* in healthy, unchallenged animals fed a basal diet consisting of relatively low amounts of fat and cholesterol compared to the average Western diet. These results suggest that genetic variation influencing T-helper effects on inflammation occurs even among healthy animals fed a non-atherogenic, basal diet. We can infer from these results that, to the extent that genetic effects on T-helper immune response influence atherosclerosis, baboons will vary in susceptibility to the development and extent of atherosclerosis. This inference is consistent with the complex nature of the pathology underlying the emergence and progression of atherosclerotic lesions observed in humans.

Based on the corresponding QTL regions inferred in the human genome, the majority of QTLs located in this study contain the gene coding for the focal transcript, a finding consistent with *cis*-regulation of expression levels for these genes in baboons. Further, for 5 of the 8 apparently *cis*-regulated QTLs located in this study, the large additive genetic variance estimated at the QTL appears to account for most or all of the total additive genetic effects on levels of the associated transcript. Although there is likely an upward bias in the estimated size of these effects[37], these initial results suggest that genetic variation at or near the coding gene exerts significant control over expression levels of many of these candidate genes, a finding in agreement with the evolutionary history of *cis*-regulation of gene expression in humans[38]. Interestingly, in agreement with results from a recent genome-wide linkage study of gene expression in human lymphocytes[27], among transcript measures in this study with overall heritability estimates ≥0.43, 60% are likely *cis*-regulated (compared to 50% in humans), and among transcript measures with overall heritability estimated at ≥0.60, 100% (compared to 80% in humans) are likely *cis*-regulated. This correspondence between findings in baboons and humans provides additional evidence that *cis* regulation of gene expression is a major determinant of transcript abundance in lymphocytes, and supports a significant degree of genetic similarity between these two species.

The extensive interdependence we observed among candidate gene transcript levels suggests that the similar degree of interaction among coded proteins revealed by network analysis (see Figure 1) may largely reflect shared, heritable variation in the expression of these genes. To assess the relevance of these findings to human atherosclerosis, we searched for published evidence of association in humans or other experimental models for each gene or gene product with lesion characteristics, risk factors for atherosclerosis, or genotypic and clinical correlates of coronary artery disease. We found reports of such associations for 32 of the 57 genes investigated (summarized in Table 3), including findings of effects at the level of the DNA sequence, the gene transcript, and the coded protein. Genetic variants in candidate genes are associated with regulation of blood pressure and susceptibility to hypertension[S23-S24], extent and severity of CAD[S25-S26], carotid artery intima-media thickness[S27], risk of myocardial infarction[S28], or established risk factors for atherosclerosis, including obesity, and CRP and triglyceride levels[S29]. Candidate genes and coded proteins are expressed/overexpressed in human and murine atheroma[8,11,19-20,24,S30-S41], associated with changes in lesion size and formation[11,24,S42-S46], and modulate cytokine levels within lesions[19,S45]. Proteins coded by candidate genes are also associated with other pathology implicated in atherosclerosis, including formation of reactive oxygen species[S44], regulation

of vascular smooth muscle cell proliferation and vasoconstrictor secretion[S38,S47-S48], and endothelial dysfunction[S31,S49-S52]. Candidate gene proteins in both membrane-bound and soluble forms are additionally upregulated in the periphery of patients with CAD[4,6,21,S37,S52-S58], particularly in patients presenting with unstable forms of disease (acute coronary syndrome)[4-6]. Moreover, it is worth noting that the protein network characterized in this study is significantly associated with autoimmune disease, particularly Type 1 diabetes and rheumatoid arthritis, both diseases featuring a substantially elevated risk of myocardial infarction due to increased atherosclerosis in patients compared to the general population[S59-S60]. It appears reasonable to infer from this collective evidence that genetic effects on pathways of Th1 and Th2 immune response influence the development and progression of atherosclerosis.

In this study, we demonstrated that quantitative genetic studies of transcripts implicated in Th1 and Th2 cell activation and function in baboons can yield valuable information about genetic effects on gene expression in associated pathways, including the extent of their interaction, chromosomal location, and likely mode of regulation. Baboons have proven to be valuable models for the study of genetic contributions to known risk factors for human atherosclerosis[S1,S61] due to their substantial genetic and physiological similarity to humans. Many of these physiological similarities are implicated in atherosclerosis, including similarities in cholesterol metabolism[S62], in endothelial cell function[S2], and in features of both fatty streak lesions that may develop under basal conditions, and of the more advanced atherosclerotic lesions that may develop under experimental conditions[S63]. These systematic similarities, combined with the ability to control dietary and other environmental variables, are likely to result in increased power to detect genetic effects on traits relevant to human disease. Further genetic studies of potential interaction between T-helper immune response traits and traditional cardiovascular risk factors in baboons may yield valuable insights into the role of adaptive immune response in the development and progression of human atherosclerosis.

Supplementary Material

Refer to Web version on PubMed Central for supplementary material.

Acknowledgments

For technical contributions and support we thank: Ms. Asia D. Mitchell, Ms. T. Baker, Ms. S. Birnbaum, Mr. J. Bridges, Ms. C. Jett, Mr. P.H. Moore, Jr., Ms. D.E. Newman, Dr. K.S. Rice, Ms. M.L. Sparks, Ms. J.F. VandeBerg, and the SNPRC veterinary and animal care staff.

Funding sources: This study was made possible by research grants from the National Institutes of Health (P01 HL028972, R01 HL068922, R01 RR008781); base grants from the National Center of Research Resources (NCRR) to the Oregon National Primate Research Center (ONPRC; P51 RR000163) and to the Southwest National Primate Research Center (SNPRC; P51 RR013986); and was conducted in facilities constructed with support from NCRR Research Facilities Improvement Program grants (C06 RR014578, C06 RR13556, C06 RR15456, C06 RR017515). Development and implementation of computational methods used in this study were supported by NIH grant MH059490, and the high-speed distributed computing facilities used for this work at the AT&T Genetics Computing Center, SFBR, were supported in part by a gift from the AT&T Foundation. The platform for lymphocyte expression profiling was supported by a generous donation from the Azar/Shepperd families, with additional funds from ChemGenex Pharmaceuticals, Ltd., Australia.

References

1. Hansson GK, Robertson AK, Soderberg-Naucler C. Inflammation and atherosclerosis. Annu Rev Pathol Mech Dis. 2006; 1:297–329.
2. Hosono M, de Boer OJ, van der Wal AC, van der Loos CM, Teeling P, Piek JJ, et al. Increased expression of T cel activation markers (CD25, CD26, CD40L and CD69) in atherectomy specimens

of patients with unstable angina and acute myocardial infarction. Atherosclerosis. 2003; 168:73–80. [PubMed: 12732389]

3. Hansson GK, Holm J, Jonasson L. Detection of activated T lymphocytes in the human atherosclerotic plaque. Amer J Pathol. 1989; 135:169–175. [PubMed: 2505620]
4. Methe H, Brunner S, Wiegand D, Nabauer M, Koglin J, Edelman ER. Enhanced T-helper-1 lymphocyte activation patterns in acute coronary syndromes. J Amer Coll Cardiol. 2005; 45:1939–1945. [PubMed: 15963390]
5. Liuzzo G, Kopecky SL, Frye RL, O'Fallon M, Maseri A, Goronzy JJ, et al. Perturbation of the T-cell repertoire in patients with unstable angina. Circulation. 1999; 100:2135–2139. [PubMed: 10571971]
6. Szodoray P, Timar O, Veres K, Der H, Szomjak E, Lakos G, et al. Th1/Th2 imbalance, measured by circulating and intracytoplasmic inflammatory cytokines – immunological alterations in acute coronary syndrome and stable coronary artery disease. Scand J Immunol. 2006; 64:336–344. [PubMed: 16918703]
7. Huber SA, Sakkinen P, David C, Newell MK, Tracy RP. T helper-cell phenotype regulates atherosclerosis in mice under conditions of mild hypercholesterolemia. Circulation. 2001; 103:2610–2616. [PubMed: 11382732]
8. Gerdes N, Sukhova GK, Libby P, Reynolds RS, Young JL, Schonbeck U. Expression of interleukin (IL)-18 and functional IL-18 receptor on human vascular endothelial cells, smooth muscle cells, and macrophages: implications for atherogenesis. J Exp Med. 2002; 195:245–257. [PubMed: 11805151]
9. Seder RA. High-dose IL-2 and IL-15 enhance the in vitro priming of naïve CD4+ T cells for IFN-γ but have differential effects on priming for IL-4. J Immunol. 1996; 156:2413–2422. [PubMed: 8786299]
10. Hansson GK, Jonasson L, Holm H, Claesson-Welsh L. Class II MHC antigen expression in the atherosclerotic plaque: smooth muscle cells express HLA-DR, HLA-DQ and the invariant gamma chain. Clin Exp Immunol. 1986; 64:261–268. [PubMed: 3527502]
11. Schreyer SA, Vick CM, LeBoeuf RC. Loss of lymphotoxin-alpha but not tumor necrosis factor-alpha reduces atherosclerosis in mice. J Biol Chem. 2002; 277:12364–12368. [PubMed: 11809756]
12. Hansson GK, Jonasson L, Lojsthed B, Stemme S, Kocher O, Gabbiani G. Localization of T lymphocytes and macrophages in fibrous and complicated human atherosclerotic plaques. Atherosclerosis. 1988; 72:135–141. [PubMed: 3063267]
13. Jonasson L, Holm J, Skalli O, Bondjers G, Hansson GK. Regional accumulation of T cells, macrophages, and smooth muscle cells in the human atherosclerotic plaque. Arteriosclerosis. 1986; 6:131–138. [PubMed: 2937395]
14. van der Wal AC, Becker AE, van der Loos CM, Das PK. Site of intimal rupture or erosion of thrombosed coronary atherosclerotic plaques is characterized by an inflammatory process irrespective of the dominant plaque morphology. Circulation. 1994; 89:36–44. [PubMed: 8281670]
15. Ovchinnikova O, Robertson AKL, Wagsater D, Folco EJ, Hyry M, Myllyharju J, et al. T-cell activation leads to reduced collagen maturation in atherosclerotic plaques of $ApoE^{-/-}$ mice. Amer J Pathol. 2009; 174:693–700. [PubMed: 19131590]
16. Benagiano M, Azzurri A, Cievo A, Amedei A, Tamburini C, Ferrari M, et al. T helper type 1 lymphocytes drive inflammation in human atherosclerotic lesions. Proc Nat Acad Sci. 2003; 100:6658–6663. [PubMed: 12740434]
17. Frostegard J, Ulfgren AK, Nyberg P, Hedin U, Swedenborg J, Andersson U, et al. Cytokine expression in advanced human atherosclerotic plaques: dominance of pro-inflammatory (Th1) and macrophage-stimulating cytokines. Atherosclerosis. 1999; 145:33–43. [PubMed: 10428293]
18. Laurat E, Poirier B, Tupin E, Caligiuri G, Hansson GK, Bariety J, et al. In vivo downregulation of T helper cell 1 immune responses reduces atherogenesis in apolipoprotein E-knockout mice. Circulation. 2001; 104:197–202. [PubMed: 11447086]
19. Uyemura K, Demer LL, Castle SC, Jullien D, Berliner JA, Gately MK, et al. Cross-regulatory roles of interleukin (IL)-12 and IL-10 in atherosclerosis. J Clin Invest. 1996; 97:2130–2138. [PubMed: 8621803]

20. Lee TS, Yen HC, Pan CC, Chau LY. The role of interleukin 12 in the development of atherosclerosis in ApoE-deficient mice. Arterioscler Thromb Vasc Biol. 1999; 19:734–742. [PubMed: 10073981]
21. Yamaoka-Tojo M, Tojo T, Inomata T, Machida Y, Osada K, Izumi T. Circulating levels of interleukin 18 reflect etiologies of heart failure: Th1/Th2 cytokine imbalance exaggerates the pathophysiology of advanced heart failure. J Card Fail. 2002; 8:21–27. [PubMed: 11862579]
22. Agnello D, Lankford CS, Bream J, Jorinobu A, Gadina M, O'Shea JJ, et al. Cytokines and transcription factors that regulate T helper cell differentiation: new players and new insights. J Clin Immunol. 2003; 23:147–161. [PubMed: 12797537]
23. Spellberg B, Edwards JE Jr. Type 1/Type 2 immunity in infectious diseases. Clin Infect Dis. 2001; 32:76–102. [PubMed: 11118387]
24. Pinderski LJ, Fischbein MP, Subbanagounder G, Fishbein MC, Kubo N, Cheroutre H, et al. Overexpression of interleukin-10 by activated T lymphocytes inhibits atherosclerosis in LDL receptor-deficient mice by altering lymphocyte and macrophage phenotypes. Circ Res. 2002; 90:1064–1071. [PubMed: 12039795]
25. Binder CJ, Hartvigsen K, Chang MK, Miller M, Broide D, Palinski W, et al. IL-5 links adaptive and natural immunity specific for epitopes of oxidized LDL and protects from atherosclerosis. J Clin Invest. 2004; 114:427–437. [PubMed: 15286809]
26. Nicholas KB, Nicholas HB Jr, Deerfield DW II. GeneDoc: analysis and visualization of genetic variation. EMBNEW NEWS. 4:14.
27. Goring HHH, Curran JE, Johnson MP, Dyer TD, Charlesworth J, Cole SA, et al. Discovery of expression QTLs using large-scale transcriptional profiling in human lymphocytes. Nat Genet. 2007; 39:1208–1216. [PubMed: 17873875]
28. Pruitt KD, Tatusova T, Maglott DR. NCBI Reference Sequence (RefSeq): a curated non-redundant sequence database of genomes, transcripts and proteins. Nucleic Acids Res. 2005; 33:D501–D504. [PubMed: 15608248]
29. Cox LA, Mahaney MC, VandeBerg JL, Rogers J. A second-generation genetic linkage map of the baboon (*Papio hamadryas*) genome. Genomics. 2006; 88:274–281. [PubMed: 16697552]
30. Almasy L, Blangero J. Multipoint quantitative-trait linkage analysis in general pedigrees. Am J Hum Genet. 1998; 62:1198–1211. [PubMed: 9545414]
31. Blangero J, Williams JT, Almasy L. Variance component methods for detecting complex trait loci. Adv Genet. 2001; 42:151–181. [PubMed: 11037320]
32. Benjamini Y, Hochberg Y. Controlling the false discovery rate: a practical and powerful approach. J R Stat Soc B. 1995; 57:289–300.
33. Mantel N. The detection of disease clustering and a generalized regression approach. Cancer Res. 1967; 27:209–220. [PubMed: 6018555]
34. Heath SC. Markov chain Monte Carlo segregation and linkage analysis for oligogenic models. Am J Hum Genet. 1997; 61:748–760. [PubMed: 9326339]
35. Ott, J. Analysis of Human Genetic Linkage. 3rd. The Johns Hopkins University Press; Baltimore, MD: 1999.
36. Feingold E, Brown PO, Siegmund D. Gaussian models for genetic linkage analysis using complete high-resolution maps of identity by descent. Am J Hum Genet. 1993; 53:234–251. [PubMed: 8317489]
37. Goring HHH, Terwilliger JD, Blangero J. Large upward bias in estimation of locus-specific effects from genomewide scans. Am J Hum Genet. 2001; 69:1357–1369. [PubMed: 11593451]
38. Ouyang C, Smith DD, Krontiris TG. Evolutionary signatures of common human cis-regulatory haplotypes. PLoS ONE. 2008; 3:e3362. [PubMed: 18846218]

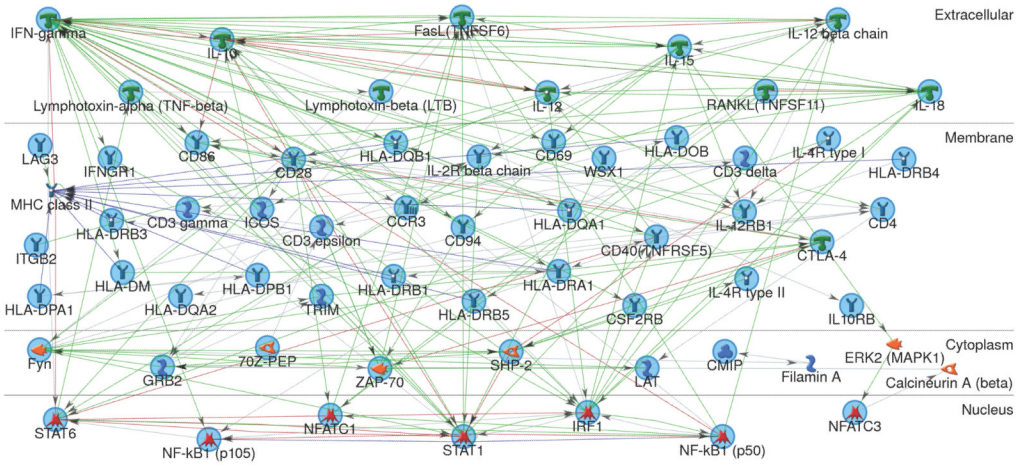

FIGURE 1.

Relationships among molecules coded by 57 focal genes, organized by cellular compartment. Network analysis was conducted using the direct-interactions building algorithm implemented in MetaCore software. = receptor ligand, = receptor, = G-protein coupled receptor, = binding protein, = complex/group of proteins, = protein kinase, = protein phosphatase, = protein, = transcription factor. Green line = upregulation, red line = down-regulation, blue line = complex or group member.

TABLE 1

Heritability of transcript levels for 57 genes implicated in pathways of Th1 and Th2 immune response: maximum likelihood estimates and associated P-values.

Transcript	h^2	P-value	Transcript	h^2	P-value
CCR3	0.138	4.26×10^{-3}	*IL2RB*	0.213	1.20×10^{-4}
CD28	0.251	7.50×10^{-6}	*IL4R*	0.243	1.36×10^{-4}
CD3D	0.278	4.72×10^{-4}	*IL10*	0.125	7.28×10^{-3}
CD3E	0.152	1.66×10^{-2}	*IL10RB*	0.166	3.25×10^{-3}
CD3G	0.388	5.73×10^{-11}	*IL12B/IL12p40*	0.120	4.76×10^{-2}
CD4	0.303	3.00×10^{-5}	*IL12RB1*	0.392	1.37×10^{-13}
CD69	0.223	1.92×10^{-3}	*IL15*	0.092	1.30×10^{-2}
CD86	0.247	8.00×10^{-7}	*IL18*	0.179	5.60×10^{-3}
CMIP	0.388	1.87×10^{-10}	*IRF1*	0.291	1.00×10^{-7}
CSF2RB	0.380	2.88×10^{-10}	*ITGB2*	0.291	1.47×10^{-8}
CTLA4	0.623	2.29×10^{-16}	*KLRD1*	0.261	2.80×10^{-6}
FYN	0.335	4.80×10^{-9}	*LAG3*	0.214	3.98×10^{-5}
GRB2	0.288	4.02×10^{-9}	*LAT*	0.143	7.76×10^{-3}
HLA-DMA	0.322	1.00×10^{-7}	*LTA/TNFB*	0.345	3.01×10^{-11}
HLA-DMB	0.353	1.60×10^{-6}	*LTB (isoform b)*	0.291	4.00×10^{-7}
HLA-DOB	0.384	3.53×10^{-8}	*NFATC1*	0.283	1.00×10^{-7}
HLA-DPA1	0.265	8.97×10^{-5}	*NFATC3*	0.239	2.00×10^{-7}
HLA-DPB1	0.276	3.50×10^{-4}	*NFKB1*	0.418	4.77×10^{-11}
HLA-DQA1	0.786	3.42×10^{-23}	*PTPN11/SHP2*	0.129	5.02×10^{-3}
HLA-DQA2	0.306	1.00×10^{-7}	*PTPN22*	0.366	4.50×10^{-9}
HLA-DQB1	0.508	9.10×10^{-14}	*STAT1*	0.310	9.64×10^{-9}
HLA-DRA	0.432	7.98×10^{-15}	*STAT6*	0.210	6.06×10^{-5}
HLA-DRB1	0.340	4.00×10^{-7}	*TNFRSF5/CD40*	0.253	8.05×10^{-5}
HLA-DRB3	0.335	8.79×10^{-5}	*TNFSF6/FASL*	0.111	3.07×10^{-2}
HLA-DRB4	0.283	2.68×10^{-5}	*TNFSF11/RANKL*	0.206	9.35×10^{-5}
HLA-DRB5	0.634	3.29×10^{-19}	*TRIM*	0.228	1.16×10^{-4}

Transcript	h^2	P-value	Transcript	h^2	P-value
ICOS	0.221	2.70×10^{-5}	*WSX1/IL27RA*	0.094	2.89×10^{-2}
IFNG	0.282	5.88×10^{-3}	*ZAP-70*	0.221	4.33×10^{-5}
IFNGR1	0.105	1.64×10^{-2}			

TABLE 2

Results of linkage analyses describing significant evidence for 14 QTLs influencing expression levels for candidate genes implicated in pathways of Th1 and Th2 immune response. Gene names in bold indicate transcript levels for which the eQTL heritability appears to account for virtually all trait heritability. Abbreviations: eQTL – expression QTL; PHA – *Papio hamadryas*; HSA – *Homo sapiens*.

Transcript	LOD	Genome-wide P-value	eQTL heritability	PHA chromosome	HSA 1.5 LOD-drop region	HSA known location	Likely regulation
CSF2RB	2.82	0.04229	0.368	10	22q11.1-22q13.31	22q13.1	*Cis*
CTLA4	4.79	0.00342	0.406	12	2q32.3-2q36.1	2q33	*Cis*
FYN	3.46	0.00883	0.331	8	8p11.21-8q22.3	6q21	*Trans*
HLA-DMA	2.76	0.04898	0.228	18	18p11.22-18q21.32	6p21.3	*Trans*
HLA-DPA1	3.12	0.02029	0.276	15	9p21.1-9q32	6p21.3	*Trans*
HLA-DQA1	14.87	1.027×10^{-14}	0.600	4	6p22.3-6p12.3	6p21.3	*Cis*
HLA-DRA	3.11	0.02079	0.314	4	6p12.1-6q24.3	6p21.3	*Trans*
HLA-DRB1	6.35	7.677×10^{-6}	0.382	4	6p22.3-6p12.3	6p21.3	*Cis*
HLA-DRB3	10.06	9.692×10^{-10}	0.399	4	6p22.3-6q12	6p21.3	*Cis*
HLA-DRB4	5.53	0.00005	0.339	4	6p24.1-6q12	6p21.3	*Cis*
HLA-DRB5	8.10	1.102×10^{-7}	0.475	4	6p22.3-6q11.1	6p21.3	*Cis*
ITGB2	3.65	0.00555	0.316	10	22q12.3-22q13.2	21q22.3	*Trans*
NFATC3	3.58	0.00658	0.266	10	22q11.23-22q13.31	16q22.2	*Trans*
STAT6	4.19	0.00148	0.252	11	12p13.1-12q23.2	12q13	*Cis*

TABLE 3

Evidence supporting association of candidate gene expression, protein, or genotypic variation with atherosclerotic lesion characteristics, systemic pathology related to atherosclerosis, risk factors for CAD, or clinical outcomes in coronary heart disease. Abbreviations: CAD – coronary artery disease, ACS – acute coronary syndrome, MI – myocardial infarction, SMC – smooth muscle cells, VSMC – vascular smooth muscle cells, PBMCs – peripheral blood mononuclear cells.

Candidate gene	Published evidence for association of candidate gene or gene product with atherosclerosis (selected references)
CCR3	Overexpressed in human atheroma[S30]
CD28	Required for T-cell response to plaque antigen(s)[S64]
CD4	Lineage marker for the majority of T-cells found in human atheroma (reviewed in [S65])
CD69	Higher percentages of T-cells with this marker found in patients with ACS and CAD than controls[6]
CD86	Upregulated in dendritic cells derived from CAD patients[S53]
CSF2RB	Codes for receptor subunit detected in cultured SMCs and endothelial and SMCs in human atheromata[S31]
CTLA4	Increased expression associated with reduced plaque size in HSP60-tolerant LDLr$^{-/-}$ mice[S32]
FYN	Polymorphisms associated with blood pressure[S23]
GRB2	Required for oxLDL uptake by macrophages and for lesion formation in mice[S42]
HLA-DRA	Expression induced in vascular endothelial cells by interferon-γ via reactive oxygen species[S49]
HLA-DRB1	Genotype associated with CAD in ACS patients and in transplantation recipients[S25]
ICOS	Expressed abundantly in plaques from ApoE-KO mice[S33]; increase in atherosclerosis in *LDLR*$^{-/-}$ mice transplanted with ICOS-deficient marrow[S43]
IFNG	Implicated in reactive oxygen species formation and lesion development (reviewed in [S44]); transcript levels are increased in the periphery of ACS patients vs. controls[4].
IL4R	Expressed in atherosclerotic plaques in both Ldlr$^{-/-}$ mice and in humans[S34]
IL10	Inhibits LDL-induced IL-12 release, overexpression decreases lesion size and complexity in LDLr$^{-/-}$ mice ([19,24]; reviewed in [S45])
IL12B/IL12p40	Expressed abundantly in human atherosclerotic plaques[19-20]; expressed in aortas of apoE-deficient mice[20]; expression in human endothelial cells attenuated via IL-10[S50]
IL15	Expressed in human and ApoE-deficient mouse atherosclerotic lesions[S35-S36]; co-localized with CD40L-positive T cells in human lesions[S35]
IL18	Present in plasma of patients presenting with myocardial ischemia[S54]; circulating levels associated with myocardial infarction and plaque area[S55], and severity of heart failure[21]
IRF1	Protein upregulated by TNFα and IFNγ, stimulating pro-atherogenic endothelin-1 release in human VSMCs[S47]; mediates apoptosis in VSMCs via PPARγ[S48]
ITGB2	Activation on T cells independently predicts severe CAD and MI[S56]
LTA/TNFB	Genotype associated with extent of coronary atherosclerosis[S26]; polymorphism associated with increased intima-media thickness of carotid artery[S27] polymorphisms associated with increased risk of myocardial infarction[S28]; present in fatty streak lesions of the aortic sinus, reduced atherosclerosis in LTα $^{-/-}$ mice[11]
NFATC1	Mediates injury-induced vascular wall remodeling[S66]
NFATC3	Changes in blood glucose are detected by NFATc3 in arterial smooth muscle, upregulating expression of osteopontin, a promoter of vascular disease[S67]

Candidate gene	Published evidence for association of candidate gene or gene product with atherosclerosis (selected references)
NFKB1	Implicated in pathways controlling lipid-dependent gene expression and lesion inflammation[S68]; stimulates upregulation of pro-atherogenic endothelin-1 release from human VSMCs[S47]; promotor polymorphisms associated with endothelial function in subjects with pre- and stage I hypertension[S24]; implicated in inflammatory gene expression and neointima formation following carotid injury in mice[S69]; increase in NF-κB activation in PBMCs and human carotid lesions[S37]
PTPN11/SHP2	Increased expression and SMC proliferation in rat aorta via pro-atherogenic advanced glycation end-product stimulation of NF-κB[S38]; part of signaling pathway regulating adhesion molecule expression in endothelial cells[S51]
PTPN22	Polymorphisms associated with carotid artery intima-media thickness and multiple risk factors for atherosclerosis in a Finnish population[S29]
STAT1	Regulates foam cell formation in vitro, and deficiency reduces lesion size in *apoe*$^{-/-}$ mice[S46]; stimulates upregulation of pro-atherogenic endothelin-1 from human VSMCs[S47]
STAT6	Differentially expressed in coronary arteries from patients with ischemic heart disease, upregulated in VSMCs of the same arteries[S39]; expression increases in human lesion-derived cells resistant to apoptosis[S40]
TNFRSF5/CD40	Expressed in human fatty streaks and complicated plaques[S41]; upregulated in dendritic cells derived from CAD patients[S53]
TNFSF6/FASL	Expression in circulating leukocytes associated with endothelial dysfunction in hyperlipidemic patients[S52]; implicated in plaque vulnerability in mice[S70]; overexpressed in PBMCs and human carotid plaques[S37]
TNFSF11/RANKL	Baseline serum levels predict CVD risk over a 15-year period in a human study population[S57]; increased T cell expression associated with unstable disease (ACS)[S58]
ZAP-70	Signal transduction in T-cells via pro-atherogenic lysophosphatidylcholine[S71]